A Comprehensive Study on Train Operation Dynamics and Passenger Comfort Optimization

Yimin Li[1(✉)] and Ruini Zhu[2]

[1] China Airport Construction Group Corporation, Beijing 100010, China
xz2646@sina.com
[2] China Tower Corporation Limited, Beijing 100142, China

Abstract. As global economic expansion fuels urban population growth and an increase in motor vehicles, the significance of urban rail trains is rising. These systems offer substantial benefits, including high capacity and speed. With the elevation in living standards, the focus has transitioned from mere transport capacity to the safety and comfort of train travel. This research utilizes a dynamic model of train operation to analyze the forces involved in the process, deriving an equation of motion on the motor side. It proposes a method for controlling the deceleration impulse rate to enhance passenger comfort. On this foundation, a load model for the train is designed and simulated. This study contributes to the field of train operation, introducing methods and models that can improve train travel, ultimately aiding in the establishment of a more sustainable, efficient, and comfortable urban transportation system.

Keywords: Electrical automation control · Deceleration impulse rate · Load model

1 Introduction

In the current era of rapid global economic expansion, we are witnessing a significant surge in urban populations and the number of motor vehicles. Amidst this backdrop, urban rail trains have emerged as a pivotal instrument in the urban rail transit system. These vehicles bring to the fore several key advantages, including a substantial carrying capacity, high speed, and a remarkable ability to avoid congestion, providing an efficient solution to the escalating urban transportation needs.

As living standards continue to ascend, societal perspectives on trains are undergoing a transformation. The focus has shifted beyond the mere transport capacity of these vehicles. This evolution in public perception and expectations calls for innovative approaches and interventions in the domain of train operation.

To address these evolving needs, our study delves into a comprehensive analysis of the forces at play during train operation. Through the utilization of a dynamic model of train operation, we engage a methodology that empowers us to deduce the equation of motion from the perspective of the motor. This equation lays a scientific groundwork for comprehending and fine-tuning the propelling forces that impel train locomotion [1].

Recognizing the pivotal role of passenger comfort in contemporary train operation, we propose a novel control method for the deceleration impulse rate. By controlling the rate at which the train decelerates, we aim to minimize sudden jolts and jerks, thereby enhancing the comfort of the ride. This aspect of our study underscores the importance of integrating passenger comfort into the broader picture of train operation efficiency and safety. Building upon the foundation of our deceleration control method, we venture further to design a load model for the train [2, 3].

Our study represents a significant stride forward in the field of train operation analysis. By introducing novel methods and models, it sets the stage for advancements in train operation. Our work contributes to the broader goal of fostering a sustainable, efficient, and comfortable urban transportation system. The insights and innovations stemming from our research have the potential to reshape the future of urban rail transit, making it more aligned with the evolving needs and expectations of urban populations.

2   Force Analysis of Train Operation Process

2.1   Adhesion Force Between Wheel and Rail

Some areas experience micro-sliding between the wheel and rail, while other areas maintain a relative velocity of 0. The region with sliding is known as the slip zone, while the region without movement is referred to as the adhesion zone. The concomitant relative deformation transpiring on the contact surface of the wheel and rail, juxtaposed with the incessant metamorphosis of the tensile and compressive states prevalent in diverse regions, engenders the transmutation of the rotational torque emanating from the propulsion device into cohesive adhesive forces [4].

There are limitations to the traction or braking forces that can be obtained by the wheel. During the motion of the train, as the wheel deftly rolls and makes contact with the rail, the contact surface segment impelled by the weight of the wheel undergoes a discernible elongation, courtesy of the frictional forces in play, while the diametrically opposed segment experiences a concurrent compressive force [5]. Throughout the train's motion, the alternating contact areas of the wheel generate the adhesive forces that the train ultimately achieves, representing the maximum traction or braking force it can obtain. If the complete expanse of the contact surface ventures into the realm of sliding, further increments in torque instigate a rupture in the adhesion bond linking the wheel and rail, thereby impeding the transmission of adhesive forces and instigating the onset of conspicuous macroscopic relative sliding [6]. The torque on the wheel cannot increase indefinitely.

From the analysis above, it is evident that the micro-sliding between the wheel and rail is crucial as it is the necessary factor for converting the wheel's driving torque into adhesion traction or braking forces.

The creep speed can be expressed as:

$$v_s = v_d - v_t \tag{1}$$

Creep rate:

$$\gamma = \frac{v_s}{v_t} = \frac{v_d - v_t}{v_t} \tag{2}$$

The adhesion coefficient:

$$\mu = \frac{F_{ad}}{F_G} \tag{3}$$

The adhesion force to each power bogie is:

$$F_{ad} = \mu M_{MG} g \tag{4}$$

The adhesion coefficient, delineating the efficacious adhesion interconnecting the wheel and rail, manifests as subject to the sway of diverse factors [7]. Throughout the operation of urban rail trains, utmost caution must be exercised to ensure that the maximum tractive force rendered by the traction motor remains well within the boundaries of the adhesion force magnitude pertinent to the corresponding conditions. Likewise, it is imperative to ensure that the maximum braking force aligns proportionally with the magnitude of the adhesion force under the prevailing circumstances, thereby precluding any likelihood of the train succumbing to a state of slippage or sliding [8].

2.2 Train Dynamic Model

Due to the high cost of traction inverters and the need to maximize the use of space within the vehicle, a pair of asynchronous motors are symmetrically mounted in parallel on the same bogie of a train, operating in unison and driven by a solitary traction inverter [9]. This arrangement allows for the efficient use of the lower space of the vehicle. The wheelsets driven by the two motors on the same bogie experience similar road conditions and have similar adhesion coefficients. Since they are driven by the same traction inverter and are in close proximity, we can consider the two motors on the same bogie as one unit and establish a model accordingly.

The total mass of each section of the bogie is:

$$F_{ad} = \mu M_{MG} g \tag{5}$$

$$M_{MG} = \frac{(M_M + M_L)}{2} \tag{6}$$

The vehicle model motion relationship:

$$J_w \frac{d\omega_d}{dt} = T_w + F_{TR} r \tag{7}$$

$$T_w = T_e R_g \tag{8}$$

$$\omega_d = \frac{v_d}{r} \tag{9}$$

The equation can also be obtained:

$$J_e \frac{d\omega_m}{dt} = T_e - T_L \tag{10}$$

$$T_L = \frac{F_{TR} r}{R_g} \tag{11}$$

3   Comfort of the Train

With social development, improvement in living standards, and the diversification of transportation options, an increasing number of people prefer more comfortable modes of travel. As a result, the comfort of riding urban rail trains has gradually become a competitive factor. Currently, the evaluation of train comfort focuses on various aspects, including longitudinal, lateral, and vertical comfort. This includes considerations such as vibration comfort, comfort during curve negotiation, and comfort during acceleration and deceleration.

3.1   Evaluation Criteria for Comfort

The daily operation of urban rail trains on regular routes can typically be categorized into four states: start-up, acceleration, coasting, and braking [10]. In the acceleration state, the traction force generated by the asynchronous motors continues to overcome resistance, resulting in a net force applied to the train. In the state of coasting, no artificial impetus or retarding force is imposed, and the train relies exclusively on its intrinsic inertia to surmount the inherent resistance. Conversely, in the state of braking, a meticulously regulated braking force is judiciously exerted to effectuate the graceful transition of the train from a state of locomotion to a state of stasis. These states have different effects on train comfort, with the start-up and braking states having significant impacts on acceleration and deceleration.

Norms such as EN13452–1 (2005) "Railway applications - Braking - Mass transit brake systems - Part 1: Performance requirements" establish explicit guidelines pertaining to trains equipped with steel wheels, outlining the permissible limits for maximum instantaneous deceleration and the maximum average deceleration impulse rate. Similarly, GB/T7928-2003 specifies requirements for the average deceleration and longitudinal shock rate for trains with semi-worn wheels traveling on dry and level tracks [11].

It is important to consider not only deceleration but also the rate of change of deceleration over time to ensure the comfort of urban rail train travel. The deceleration impulse rate, denoting the temporal derivative of deceleration, emerges as a paramount parameter in appraising the operational comfort of trains, thereby engendering escalating scrutiny and interest.

3.2   Deceleration Impulse Rate

For passengers, comfort can be measured by the magnitude of the impact experienced during train travel. The impulse rate, also known as the deceleration impulse rate, represents the magnitude of the deceleration impulse.

The following is the equation for discomfort while driving:

$$\sum_t Jerk = \int \left| \frac{d\beta}{dt} \right| dt \tag{12}$$

When the value of *Jerk* is smaller, it indicates that the train experiences less impact throughout the entire travel process, resulting in higher overall comfort. When the value

of *Jerk* is below a certain threshold, its impact on passengers can be considered negligible and within an acceptable range, as follows:

$$\begin{cases} Comfortable = J_0\left(\sum_t Jerk \leq J_H\right) \\ Comfortable = f\left(Jerk\right)\left(\sum_t Jerk > J_H\right) \end{cases} \tag{13}$$

The function $f\left(Jerk\right)$ decreases as *Jerk* increases.

Although the introduction of jerk control in the control method theoretically allows for adjusting the comfort during braking, in most practical engineering projects that adopt the electric-air composite braking mode, nonlinear variations in the friction coefficient of the brake pads and velocity measurement errors can lead to the transition from electric braking to air braking at low speeds, which continues until the train comes to a complete stop. This prevents the precise control of jerk during deceleration.

4   Analysis of the Entire Train Operation Process

Figure 1 unveils an illustrative diagram, intricately unraveling the comprehensive sequence of urban rail train operation. The temporal dimension is elegantly captured along the horizontal axis, while the vertical axis artfully portrays the frequency domain, collectively capturing a snapshot of the train's meticulous station entry and exit maneuvers.
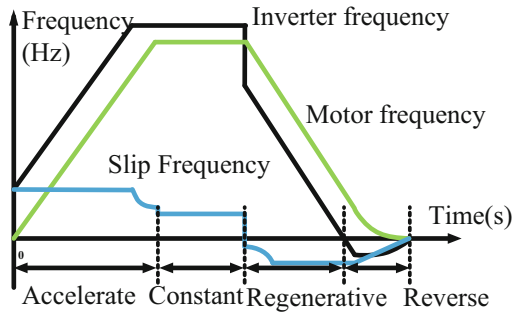

Fig. 1. The whole process of train operation

During the acceleration and start-up phase, the asynchronous electric motors operate in traction mode, maintaining a slip frequency above 0. The stator frequency outpaces the rotor frequency, which results in an electromagnetic force that propels the train forward as traction force.

Following a period of steady-state operation, the train transitions into the braking phase. Initially, regenerative braking is utilized. The asynchronous electric motors shift into generator mode, maintaining a slip frequency below 0. Here, the electromagnetic force is exerted as a braking force.

As the train decelerates and the stator frequency approaches 0, the asynchronous electric motors are unable to sustain regenerative braking. To uphold an adequate electric

braking force, it becomes imperative to alter the phase sequence of the inverter's three-phase power supply. Subsequently, the slip frequency exceeds 1, and the braking state transitions to plugging braking. This change allows the asynchronous electric motors to draw energy from the inverter, continuing to produce an electromagnetic force opposing their rotation.

During the transition between braking states, careful measures must be taken to prevent issues such as current surges caused by the switch from regenerative to plugging braking. An optimal solution is to control the slip frequency to switch at the natural commutation point, allowing the stator frequency to cross 0 Hz automatically.

During the ultimate stage of braking, expeditiously implementing the parking brake and ceasing the application of electric braking force assumes paramount significance. Failure to do so could potentially result in reverse acceleration of the train, posing serious safety risks.

5 Simulation Verification

The basic configuration of the train consists of a $3 + 3$ power unit arrangement, with a total of 6 cars. To reduce costs associated with traction inverters, each motor car is equipped with two inverters. Moreover, a pair of asynchronous motors are symmetrically positioned in parallel on the identical bogie of the motor car, seamlessly driven by a solitary traction inverter in Fig. 2.

Fig. 2. Train marshalling

The obtained ideal torque is then combined with the basic resistance of the train to calculate the real-time acceleration (deceleration). The integration of acceleration yields the real-time running speed of the train, enabling the simulation to dynamically track the variations in parameters throughout the train's operation. The simulation input entails the rotor angular speed, accurately simulating the train's operational state. The schematic representation of the simulation testing's design approach is eloquently showcased in Fig. 3.
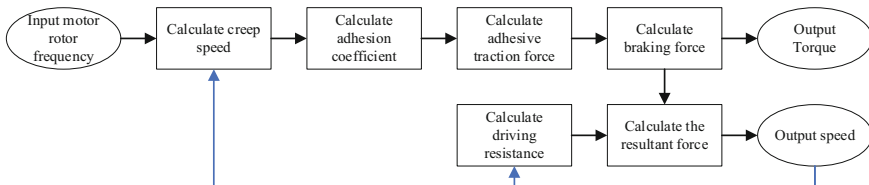

Fig. 3. Design for simulating the running process

The simulation module meticulously emulates the train's acceleration and deceleration, vividly demonstrated in Fig. 4. The train embarks on an acceleration phase,

gracefully surging from 0 km/h to 30 km/h, followed by a subsequent deceleration phase, seamlessly returning to a standstill at 0 km/h.
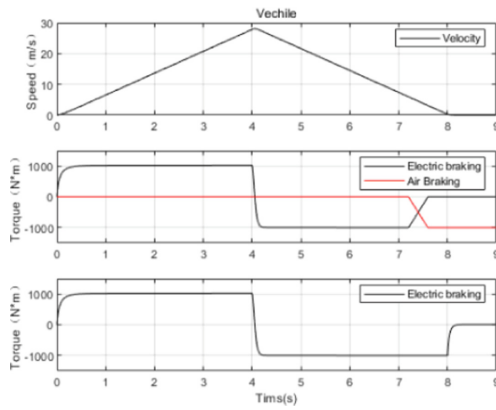

Fig. 4. Model running simulation

During the train's acceleration process, the asynchronous motors operate in traction mode, providing traction force. In this mode, the module outputs positive torque. As the train undergoes the deceleration process, it seamlessly transitions into the regenerative braking phase, characterized by the electric-air composite braking mode. Within this mode, the asynchronous motors seamlessly operate in the braking mode, yielding a reverse braking force to facilitate the deceleration. In this mode, the module outputs negative torque. As the speed gradually reaches the threshold of 8 km/h, the electric-air composite braking mode is engaged, wherein the electric braking force experiences a decrement while the air braking force augments correspondingly, assuring dependable braking performance. Subsequently, during the full electric braking mode, the electric braking force diligently endures as the predominant means of generating braking power, steadfastly exerting its maximum potential until the inverter is ultimately deactivated upon reaching the speed threshold of 0.5 km/h. From that point onward, the train relies on inertia to gracefully come to a halt. Throughout this entire sequence, stringent control of the deceleration impulse rate is implemented to enhance the operational comfort of the train.

6   Conclusion

This chapter investigated the forces experienced during train operation, analyzed the comfort aspects and evaluation metrics, designed a corresponding deceleration impulse rate control method, and developed a load model for the train with simulation verification. This research contributes to the field of train operation by designing a load model for train operation, which helps in establishing a more sustainable, efficient, and comfortable urban transportation system.

References

1. Wu, C., Lu, S., Xue, et al.; A Two-step method for energy-efficient train operation, timetabling and on-board energy storage device management. IEEE Trans. Transp. Electrification (99), 1–1 (2021). https://doi.org/10.1109/TTE.2021.3059111

2. Yong, P., Jiahao, Z., Chaojie, F., et al.: A review of passenger ride comfort in railway: assessment and improvement method. Transp. Safety Environ. **2**, 2 (2022). https://doi.org/10.1093/tse/tdac016

3. Ahmed, A.A., Masood, M.A., Almabrouk, A.Q., et al.: An investigation of the effect of the hub motor weight on vehicle suspension and passenger comfort. J. Automob. Eng. (11–2) (2021). https://doi.org/10.24247/ijmperdoct 20214

4. Fort, A., Landi, E., Mugnaini, M., et al.: Real time car passengers comfort monitoring by means of environmental and vibrational measurements. In: 2021 IEEE international workshop on metrology for automotive (MetroAutomotive). IEEE (2021). https://doi.org/10.1109/MetroAutomotive50197. 2021.9502860

5. Gao, B., Zheng, K., Zhang, F., Su, R., Zhang, J., Wu, Y.: Research on multi-target tracking method based on multi-sensor fusion. Smart and Resilient Transp. **4**(2), 46–65 (2022). https://doi.org/10.1108/SRT-05-2022-0010

6. Sciencetechnology, D.O., Graduate School of Sophia University, Sciences, E.A., et al.: Study on modeling and numerical analysis for the prediction of wheel wear development. Mech. Eng. J. (2017). https://doi.org/10.1299/mej.17-00126

7. Wu, B., Wen, Z., Wang, H., et al.: Analysis of wheel/rail adhesion under oil contamination with surface roughness. Proc. Inst. Mech. Eng. Part J J. Eng. Tribol. **227**(11), 1306–1315 (2013). https://doi.org/10.1177/1350650113491866

8. Zerzeri, M., Khedher, A.: Optimal speed–torque control of doubly-fed induction motors: analytical and graphical analysis. Comput. Electr. Eng. **93**(2), 107258 (2021). https://doi.org/10.1016/j.compeleceng.2021.107258

9. Kawamura, N., Zanma, T., Koiwa, K., et al.: Simultaneous estimation of rotor speed and stator resistance in speed-sensorless vector control of IMs. IEEE J. Indus. Appl. (2021). https://doi.org/10.1541/ieejjia.20011814

10. Xiu, C., Yao, F., Zheng, J.: Comparative analysis of two speed-estimation methods for dual three-phase induction motor with stator resistance online identification. Electronics **10**(23), 2951 (2021). https://doi.org/10.3390/electronics10232951

11. Wu, S., Li, Y., Zheng, Z.: Speed sensorless vector control of induction motor based on full-order flux observer. In: IEEE international power electronics & motion control conference. IEEE (2009).https://doi.org/10.1109/IPEMC.2006.4778330